Proc. Indian Acad. Sci. (Chem. Sci.), Vol. 104, No. 3, June 1992, pp. 351–360.

Manganese(III)-carboxylate binding: Chemistry and structure of a hydrated pyridinedicarboxylate

SWAPAN KUMAR CHANDRA, PARTHA CHAKRABORTY and ANIMESH CHAKRAVORTY*

Department of Inorganic Chemistry, Indian Association for the Cultivation of Science, Calcutta 700032, India

MS received 25 November 1991

Abstract. The reaction of $Mn(CH_3COO)_3 \cdot 2H_2O$ with the carboxyl-rich ligand pyridine-2,6-dicarboxylic acid (H_2L) in methanol affords a high-spin ($S = 2$) hydrated *bis*-complex. Structure determination has revealed the solid to be $[Mn^{III}(H_2L)(L)][Mn^{III}L_2] \cdot 5H_2O$: space group $P\bar{1}$; $Z = 2$; $a = 7{\cdot}527(3)$ Å, $b = 14{\cdot}260(4)$ Å, $c = 16{\cdot}080(6)$ Å, $\alpha = 91{\cdot}08(3)°$, $\beta = 103{\cdot}58(3)°$, $\gamma = 105{\cdot}41(3)°$ and $V = 1611{\cdot}2(10)$ Å^3. Each ligand is planar and is bonded in the tridentate O_2N fashion. The MnO_4N_2 coordination spheres show large distortions from octahedral symmetry. The lattice is stabilised by an extensive network of O...O hydrogen-bonding involving water molecules and carboxyl functions. Upon dissolution in water, protic redistribution occurs and the complex acts as the mono-basic acid Mn(HL)(L) (pK, $4{\cdot}3 \pm 0{\cdot}05$). The deprotonated complex displays high metal reduction potentials: $Mn^{IV}L_2$–$Mn^{III}L_2^-$, 1·05 V; $Mn^{III}L_2^-$–$Mn^{II}L_2^{2-}$, 0·28 V vs. SCE.

Keywords. Manganese(III) pyridinedicarboxylate; metal reduction potential; protic redistribution.

1. Introduction

This work stems from our interest in the chemistry of manganese in biomimetic environments (Chandra *et al* 1990a, 1990b; Chandra and Chakravorty 1991). Manganese–carboxylate binding has been strongly implicated in the photosystem II (Dismukes 1988; Christou 1989; Guiles *et al* 1990) and this is a plausible origin of the high metal reduction potential required for water oxidation (Dutta *et al* 1991). In this context synthetic complexes of manganese with carboxyl-rich ligands are of interest. A model ligand of this class is pyridine-2,6-dicarboxylic acid (H_2L). The synthesis and electrochemistry of a few manganese complexes of H_2L have received attention (Yamaguchi and Sawyer 1985; Nathan *et al* 1989) but none of these has been structurally characterised. In the present work we describe a new complex whose structure determination has revealed it to be $[Mn(H_2L)(L)][MnL_2] \cdot 5H_2O$. Upon dissolution in water, protic redistribution occurs. Metal reduction potentials are high.

*For correspondence

2. Experimental

2.1 *Materials and preparation of* $[Mn(H_2L)(L)][MnL_2]\cdot 5H_2O$

$Mn(CH_3COO)_3\cdot 2H_2O$ was prepared as reported (Brauer 1965). All other chemicals and solvents were of analytical grade and used as received.

To a solution of pyridine-2,6-dicarboxylic acid (H_2L, 0·70 g, 4·18 mmol) in methanol (40 ml) was added solid $Mn(CH_3COO)_3\cdot 2H_2O$ (0·55 g, 2·05 mmol). The mixture was magnetically stirred for one hour. The filtrate was allowed to evaporate slowly at room temperature. Red-brown prismatic crystals were formed over 4–5 days; yield 0·75 g (~ 85%).

2.2 *Physical measurements*

Magnetic susceptibility was measured on a PAR-155 vibrating-sample magnetometer fitted with a Walker Scientific L75FBAL magnet. Electrochemical measurements were performed on a PAR Model 370-4 electrochemistry system. A Perkin-Elmer 240C elemental analyzer was used to collect microanalytical data (C, H, N). Acid base titrations were carried out in a nitrogen atmosphere by using a Systronics, India, pH meter.

2.3 *Determination of pKa*

A solution of 0·00704 g of the complex is 25 ml water was titrated pH-metrically with $1{\cdot}34 \times 10^{-2}$ N carbonate-free NaOH. The pH was then plotted against $\log[\bar{h}/(1-\bar{h})]$ as defined below,

$$\mathrm{pH} = pK_a + \log[\bar{h}/(1-\bar{h})], \tag{1}$$

where $\bar{h} = [Na^+]/c$; $[Na^+]$ is the concentration of Na^+ and c is the total concentration of acid. The value of the pK_a is the intercept of the linear plot. Addition of excess alkali leads to decomposition of the complex with precipitation of insoluble hydrous manganese oxide.

2.4 *X-ray structure determination*

Single crystals of the complex were grown by slow evaporation of methanol solution of the compound. A red-brown prismatic crystal ($0{\cdot}12 \times 0{\cdot}19 \times 0{\cdot}24\ mm^3$) was mounted on a glass fibre. Data collection was performed on a Nicolet R3m/V automated diffractometer using graphite-monochromated MoK_α radiation ($\lambda = 0{\cdot}71073$). The unit cell parameters were determined by least-squares fit of 18 reflections (selected from a rotation photograph) having 2θ values in the range 5–24°. Lattice dimensions and the Laue group were checked by axial photography. The structure was successfully solved in the space group $P\bar{1}$ using 4359 ($I > 3\sigma(I)$) out of the total 7173 independent reflections ($2° \leqslant 2\theta \leqslant 55°$).

During data collection the parameters kept fixed were as follows: $\theta - 2\theta$ scan mode with scan range of 1·40°; variable scan speed between 3·0 and 30·0° min^{-1}; ratio of background/scan time 0·5. Two check reflections were measured after every 98 reflections to monitor crystal stability. No significant intensity reduction was observed

in the 110 h of exposure to X-rays. Data were corrected for Lorentz-polarization effects and an empirical absorption correction was done on the basis of azimuthal (North *et al* 1968) scans of six reflections with χ ranging from 284–288° and 75–81° and 2θ in the range 11–34°.

All calculations for data reduction, structure solution, and refinement were done on a MicroVAX II computer with the programs of SHELXTL-PLUS (Sheldrick 1988). The structure was solved by direct methods. The model was then refined by full-matrix least-squares procedures. All non-hydrogen atoms were refined anisotropically. Hydrogen atoms were then included at their idealised positions with fixed-thermal parameters. No correlations were observed in the final refinement, and the highest difference Fourier Peak was 0·54e/Å^3. Further details can be obtained by writing to the authors.

3. Results and discussion

3.1 *Synthesis and characterisation*

The reaction of manganese(III) acetate dihydrate with H_2L in aqueous methanol affords in good yield red-brown crystals of the complex (1) having the composition $MnHL_2 \cdot 2{\cdot}5H_2O$. The monohydrate $MnHL_2 \cdot H_2O$ has been reported (Yamaguchi and Sawyer 1985) to be formed in acetonitrile solvent but we have not encountered it in our work.

Selected characterisation data for 1 are listed in table 1. The complex is virtually nonconducting in methanol solution but has good conductivity (Λ_m at 300 K, 312 ohm^{-1} cm^2 mol^{-1} in $\sim 10^{-3}$ M solution) in aqueous solutions due no doubt to protic dissociation, *vide infra*. It has four unpaired electrons corresponding to high-spin manganese(III) and it is expectedly ESR-silent. In O_h symmetry high-spin manganese(III) is expected to have only one spin allowed ligand field transition but (1) displays several (table 1) in qualitative agreement with the distortion of the manganese(III) environment (see below).

3.2 *Structure*

Selected crystal data and data collection parameters are listed in table 2. Atomic coordinates and isotropic equivalent thermal parameters are collected in table 3. The asymmetric unit of the crystal consists of two independent *bis* chelated manganese

Table 1. Analytical, magnetic moment[a], and electronic spectral data for $[Mn(H_2L)(L)] \cdot [MnL_2] \cdot 5H_2O$.

Elemental analysis (%)[b]				μ_{eff}/Mn	UV-Vis-near-IR spectral data/Mn
C	H	N	Mn	(B M)	λ_{max}/nm(ε/M^{-1} cm^{-1})
38·88 (38·98)	2·72 (2·78)	6·49 (6·49)	12·76 (12·74)	4·93	480(260)[c,d], 510(320)[c], 690(120)[c], 1000(60)[c,d], 472(170)[d,e], 497(190)[e], 1000(90)[e]

[a]In the solid state at 298 K; [b]calculated values are in parentheses; [c]in methanol at 298 K; [d]shoulder; [e]in water at 298 K.

Table 2. Crystallographic data for $[Mn(H_2L)(L)][MnL_2]\cdot 5H_2O$.

Formula	$C_{28}H_{24}N_4O_{21}Mn_2$
Formula weight	862·4
Crystal size, mm^3	0·12 × 0·19 × 0·24
Crystal system	Triclinic
Space group	$P\bar{1}$
a, Å	7·527(3)
b, Å	14·260(4)
c, Å	16·080(6)
α, (degrees)	91·08(3)
β, (degrees)	103·58(3)
γ, (degrees)	105·41(3)
V, $Å^3$	1611·2(10)
Z	2
No. of centring reflections	18
Centring 2θ, (degrees)	5–24
D_c, g/cm^{-3}	1·77
$\mu(M_oK_\alpha)$, cm^{-1}	8·49
2θ, limits, (degrees)	2–55
No. of unique reflections	7173
Observed data $I > 3\sigma(I)$	4359
Parameters refined	496
R^a, %	6·53
R_w^b, %	7·21
g in weighting scheme[c]	0·0005
Largest peak in final Fourier map, $e/Å^3$	0·54

[a] $R = \Sigma||F_o| - |F_c||/\Sigma|F_o|$. [b] $R_w = [\Sigma w(|F_o| - |F_c|)^2/\Sigma w|F_o|^2]^{1/2}$: [c] $1/[\sigma^2(|F_o|) + g|F_o|^2]$.

Table 3. Atomic coordinates ($\times 10^4$) and equivalent isotropic displacement coefficients ($Å^2 \times 10^3$) for $[Mn(H_2L)(L)][MnL_2]\cdot 5H_2O$[a].

Atom	x	y	z	U(eq)
Mn(1)	4079(1)	2373(1)	5726(1)	28(1)
N(1)	3202(6)	949(3)	5258(3)	24(1)
O(5)	6721(6)	2569(3)	6393(3)	35(1)
O(3)	2921(6)	1607(3)	6712(3)	36(1)
O(4)	1372(6)	145(3)	7017(3)	42(2)
O(1)	4961(6)	2389(3)	4560(3)	35(1)
O(7)	1694(6)	2669(3)	5213(3)	41(2)
N(2)	4836(7)	3769(3)	6038(3)	27(2)
Mn(2)	3701(1)	7281(1)	594(1)	30(1)
N(4)	4956(6)	8732(3)	932(3)	27(2)
O(14)	1640(6)	8999(3)	2060(3)	43(2)
N(3)	2798(6)	5905(3)	181(3)	25(1)
O(9)	1967(6)	7345(3)	−485(3)	36(2)
O(8)	346(6)	3884(3)	4910(3)	52(2)
O(6)	9403(6)	3696(3)	7050(3)	46(2)
O(2)	4959(6)	1441(3)	3437(3)	40(2)
O(15)	6086(6)	7628(3)	20(3)	39(2)
O(16)	8284(7)	8860(3)	−291(3)	53(2)
O(12)	5516(7)	5352(3)	2075(3)	45(2)

(*Continued*)

Table 3. (*Continued*)

Atom	*x*	*y*	*z*	*U*(eq)
O(11)	4886(6)	6716(3)	1581(3)	40(2)
O(10)	139(7)	6474(3)	−1708(3)	51(2)
O(13)	1943(6)	7726(3)	1333(3)	40(2)
C(13)	3547(8)	4256(4)	5753(3)	30(2)
C(1)	4531(8)	1588(4)	4108(3)	28(2)
C(9)	6618(9)	4199(4)	6443(3)	31(2)
C(3)	2787(8)	−233(4)	4134(3)	30(2)
C(7)	2186(8)	680(4)	6561(3)	29(2)
C(14)	1672(9)	3589(4)	5254(4)	35(2)
C(12)	4083(10)	5273(4)	5907(4)	36(2)
C(5)	1667(8)	−696(4)	5391(4)	31(2)
C(8)	7715(9)	3449(4)	6663(3)	33(2)
C(2)	3438(7)	712(4)	4494(3)	25(2)
C(6)	2361(7)	271(4)	5719(3)	24(2)
C(11)	5950(10)	5735(4)	6324(4)	40(2)
C(4)	1897(8)	−950(4)	4587(4)	31(2)
C(10)	7250(10)	5192(4)	6613(4)	40(2)
C(22)	2462(8)	8603(4)	1611(3)	31(2)
C(19)	2963(9)	4312(4)	370(4)	34(2)
C(16)	1673(8)	5663(4)	−614(3)	27(2)
C(20)	3452(7)	5270(4)	678(4)	26(2)
C(23)	4220(8)	9233(4)	1401(3)	29(2)
C(15)	1182(8)	6548(4)	−998(4)	33(2)
C(17)	1141(8)	4714(4)	−965(4)	34(2)
C(27)	6465(8)	9184(4)	648(3)	29(2)
C(21)	4723(8)	5785(4)	1516(3)	31(2)
C(18)	1795(8)	4025(4)	−458(4)	35(2)
C(28)	7021(8)	8504(4)	80(4)	34(2)
C(26)	7329(8)	10176(4)	839(4)	35(2)
C(25)	6572(9)	10704(4)	1341(4)	36(2)
C(24)	4996(9)	10219(4)	1625(3)	33(2)
O(1W)	8148(7)	2760(3)	3323(3)	49(2)
O(2W)	599(6)	1773(3)	2844(3)	48(2)
O(3W)	2444(8)	2099(4)	1692(3)	68(2)
O(4W)	5685(7)	3419(3)	2054(3)	49(2)
O(5W)	−969(6)	7733(3)	2333(3)	46(2)

[a]Equivalent isotropic *U* defined as one third of the trace of the orthogonalized U_{ij} tensor

atoms and five independent water molecules (figure 1). The composition of the asymmetric unit is thus twice that of the empirical composition. An extensive network of water–water and water–carboxyl hydrogen bonds is present (figure 2). Selected bond distances and angles are listed in table 4 and significant hydrogen bonded O...O distances are given in table 5. Each ligand binds the metal in tridentate O_2N mode and each MnL fragment is excellently planar (mean deviation, 0·02–0·04 Å). The Mn(1)...Mn(2) distance is 10·922(2)Å.

The MnO_4N_2 coordination spheres show large deviations from idealized geometry. Good indicators of this are the angles (value in O_h 180·0°) subtended at the metal centre by donor atoms *trans* to each other e.g., N(1)–Mn(1)–N(2), 173·5(2)°,

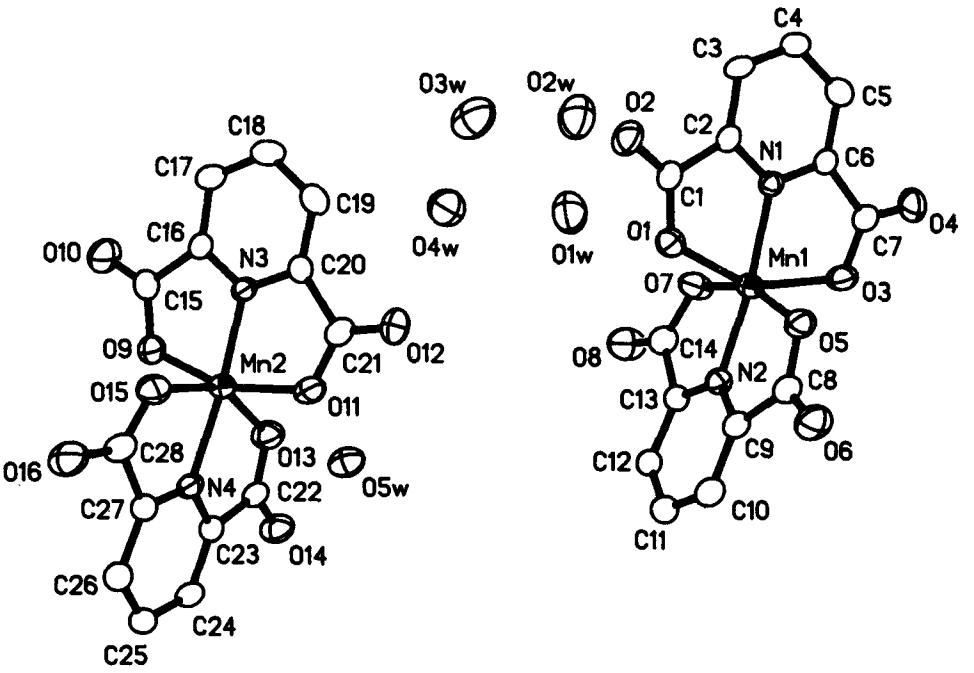

Figure 1. ORTEP plot and labelling scheme for $[Mn(H_2L)(L)][MnL_2]\cdot 5H_2O$. All atoms are represented by their 50% probability ellipsoids.

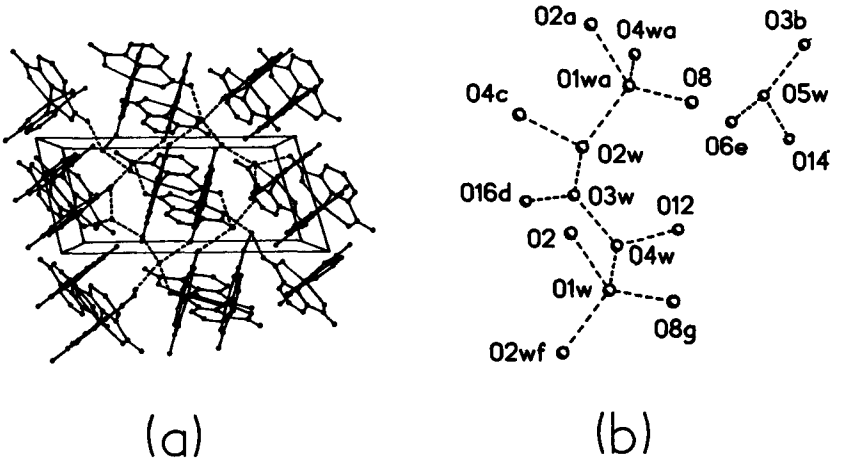

Figure 2. (a) Packing diagram viewed along *b*-axis. (b) Pattern of hydrogen bonding.

O(1)–Mn(1)–O(3), 151·5(2)° and O(5)–Mn(1)–O(7), 159·5(2)°. Another manifestation of distortion is the pronounced inequality of the interaction of the two ligands with the metal atom within each *bis* chelate molecule. Thus the Mn(1)–O and Mn(1)–N distances corresponding to the two ligands in the molecule containing Mn(1) differ by as much as 0·2 and 0·1 Å respectively.

The C–O distances show a significant trend. Let O_b and O_n be oxygen atoms bonded and nonbonded to the metal atom. In six of the eight carboxyl groups the

Table 4. Selected bond distances (Å) and angles (degrees) and their estimated standard deviations for $[Mn(H_2L)(L)][MnL_2]\cdot 5H_2O$[a].

Distances			
Mn(1)–N(1)	2·031(4)	Mn(2)–N(3)	1·944(4)
Mn(1)–N(2)	1·940(4)	Mn(2)–N(4)	2·036(4)
Mn(1)–O(1)	2·129(5)	Mn(2)–O(9)	1·931(4)
Mn(1)–O(3)	2·162(4)	Mn(2)–O(11)	1·931(4)
Mn(1)–O(5)	1·968(4)	Mn(2)–O(13)	2·174(5)
Mn(1)–O(7)	1·950(5)	Mn(2)–O(15)	2·155(5)
C(1)–O(1)	1·265(6)	C(15)–O(9)	1·303(6)
C(1)–O(2)	1·228(8)	C(15)–O(10)	1·210(7)
C(7)–O(3)	1·284(6)	C(21)–O(11)	1·300(7)
C(7)–O(4)	1·216(7)	C(21)–O(12)	1·229(7)
C(8)–O(5)	1·285(6)	C(22)–O(13)	1·246(7)
C(8)–O(6)	1·228(7)	C(22)–O(14)	1·266(8)
C(14)–O(7)	1·317(7)	C(28)–O(15)	1·250(6)
C(14)–O(8)	1·205(8)	C(28)–O(16)	1·240(8)
Angles			
N(1)–Mn(1)–O(1)	76·0(2)	N(3)–Mn(2)–O(9)	80·0(2)
N(1)–Mn(1)–O(3)	75·8(2)	N(3)–Mn(2)–O(11)	79·6(2)
N(2)–Mn(1)–O(5)	79·3(2)	N(4)–Mn(2)–O(13)	75·2(2)
N(2)–Mn(1)–O(7)	80·3(2)	N(4)–Mn(2)–O(15)	75·3(2)
N(1)–Mn(1)–N(2)	173·5(2)	N(3)–Mn(2)–N(4)	171·5(2)
O(1)–Mn(1)–O(5)	90·4(2)	O(9)–Mn(2)–O(13)	92·4(2)
O(3)–Mn(1)–O(7)	92·1(2)	O(11)–Mn(2)–O(15)	96·9(2)
O(1)–Mn(1)–O(7)	94·8(2)	O(9)–Mn(2)–O(15)	91·4(2)
O(3)–Mn(1)–O(5)	92·7(2)	O(11)–Mn(2)–O(13)	89·9(2)
O(1)–Mn(1)–O(3)	151·5(2)	O(9)–Mn(2)–O(11)	158·6(2)
O(5)–Mn(1)–O(7)	159·5(2)	O(13)–Mn(2)–O(15)	150·5(1)

[a]Numbers in parentheses are estimated standard deviations in the least significant digits.

Table 5. Hydrogen-bonded O...O distances (Å)[a].

O1w...O2wf	2·825(6)	O2w...O4c	2·784(5)
O1w...O8g	2·808(6)	O2w...O1wa	2·825(9)
O1w...O2	2·674(8)	O1wa...O8	2·876(6)
O1w...O4w	2·776(7)	O1wa...O2a	2·674(8)
O4w...O12	2·793(9)	O1wa...O4wa	2·776(7)
O4w...O3w	2·585(8)	O5w...O3b	2·672(8)
O3w...O16d	2·480(8)	O5w–O14	2·420(7)
O3w...O2w	2·545(5)	O5w...O6e	2·708(6)

[a]In relation to coordinates of table 3, the coordinates of atoms marked as a, b etc. here are: a, $x-1$, y, z; b, $-x$, $-y+1$, $-z+1$; c, $-x$, $-y$, $-z+1$; d, $-x+1$, $-y+1$, $-z$; e, $-x+1$, $-y+1$, $-z+1$; f, $x+1$, y, z; g, $1-x$, y, z.

C–O lengths follow the order $C–O_b > C–O_n$, (2). This is expected for monodentate deprotonated carboxyl functions. The average $C–O_b$ and $C–O_n$ distances are 1·292(7)Å and 1·219(8)Å respectively. The two exceptional carboxyl groups are C(22)O(13)O(14) and C(28)O(15)O(16) which belong to one ligand bonded to Mn(2).

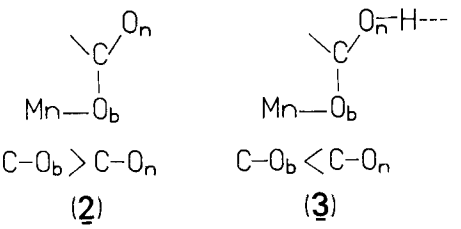

(2) (3)

Here, $C-O_b \leqslant C-O_n$ and the two O_n atoms, O(14) and O(16), are involved in very short (< 2·5 Å) O...O hydrogen bonds (table 5). This behaviour is diagnostic (Quaglieri and Thomas 1972; Loiseleur 1973) of monodentate, undissociated carboxyl functions involved in hydrogen bonding, (3). Thus the Mn(1) and Mn(2) chelates occur as MnL_2^- and $Mn(H_2L)(L)^+$, respectively, and the crystalline complex can be formulated as $[Mn(H_2L)(L)][MnL_2]\cdot 5H_2O$. We comment on this point further in the next section.

The structures of a few metal complexes of H_2L are known. Among *bis* complexes of *3d* ions the two ligands are equivalent in $Rb[CrL_2]$ (Fürst *et al* 1979) and they are nearly so in $[Ni(HL)_2]\cdot 3H_2O$ (Quaglieri and Thomas 1972). In $[Cu(H_2L)(L)]\cdot 3H_2O$ (Loiseleur 1973) as well as in $[Ag(H_2L)(L)]\cdot H_2O$ (Drew *et al* 1970) the two ligands bind in a grossly unequal fashion. Our manganese(III) complex also belongs to this category. Interestingly the cation Cu^{2+}, Ag^{2+} and Mn^{3+} are all Jahn–Teller active under octahedral coordination but Cr^{3+} and Ni^{2+} are not.

Water molecules of type 01w–04w form an infinite hydrogen-bonded chain to which carboxyl oxygen atoms are associated (figure 2). Water of type 05w stands isolated with associated carboxyl oxygen neighbours. All water molecules except O1w form three hydrogen bonds; 01w forms four. Among carboxyl oxygen atoms all O_n atoms except O(10) are hydrogen bonded. Among O_b atoms only O(3) is so bonded. It is evident from the structure that an organised carboxyl-rich environment is able to hold multiple water molecules in close association.

3.3 *Solution chemistry*

In aqueous solution (1) behaves as a monobasic acid as per the equation below. From pH-metric titration with NaOH, the pK_a of the acid is found to be

$$[Mn(HL)(L)] \overset{K_a}{\rightleftharpoons} [MnL_2]^- + H^+, \tag{2}$$

4·30 ± 0·05 at 298 K. This value is smaller than that of uncoordinated HL^- (4·68, Martell and Smith 1974), as expected. The dissolution of the crystalline complex in water is thus attended with protic redistribution,

$$[Mn(H_2L)(L)][MnL_2] \xrightarrow{\text{dissolve}} 2[Mn(HL)(L)], \tag{3}$$

followed by acid dissociation, (2). Recrystallisation reverses the process of (3). The feasibility of generating the cation $[Mn(H_2L)(L)]^+$ from [Mn(HL)(L)] by addition of acid in solution was investigated. No pH-metric evidence for such proton association

could however be found implying that $[Mn(H_2L)(L)]^+$ is a strong acid. The first dissociation constant (pK_a) of uncoordinated H_2L is 2·10 (Martell and Smith 1974); coordination to a trivalent metal is indeed expected to make H_2L a strong acid.

The transformation in (3) can be visualized as the thermodynamically favourable proton transfer from the strong acid $[Mn(H_2L)(L)]^+$ to the relatively weak base $[MnL_2]^-$ in mobile solution. Formally it can be viewed as protic comproportionation, its reversal by crystallization corresponding to protic disproportionation. The stable coexistence of the acid–base pair in the crystalline state is a good example of how the relatively rigid lattice forces can modify chemistry. The regiospecific hydrogen-bonded network is no doubt an important constituent of such forces here.

The couples $[Mn^{VI}L_2]/[Mn^{III}L_2]^-$ and $[Mn^{III}L_2]^-/[Mn^{II}L_2]^{2-}$ have already been reported for acetonitrile solutions of $[MnL_2]^-$ (Yamaguchi and Sawyer 1985). Upon neutralisation of the dissociable proton with tetrabutyl ammonium hydroxide in acetonitrile, (1) behaves similarly. The quasireversible one-electron cyclic voltammetric responses corresponding to the above two couples are observed. The peak-to-peak separations lie in the range 80–100 mV and the formal potentials are: Mn^{III}/Mn^{II}, 0·28 V and Mn^{IV}/Mn^{III}, 1·05 V vs saturated calomel electrode. The relatively high potentials are consistent (Dutta *et al* 1991) with the carboxyl-rich environment. Indeed four-fold carboxyl coordination to the metal in (1) has raised the Mn^{IV}/Mn^{III} reduction potential beyond the water oxidation threshold.

4. Conclusions

A manganese(III) complex of pyridine-2,6-dicarboxylic acid (H_2L) has been structurally characterised for the first time. The crystalline complex has the formulation $[Mn(H_2L)\cdot(L)][MnL_2]\cdot 5H_2O$. Both the MnO_4N_2 coordination spheres are highly distorted. The lattice is stabilised by extensive water–water and water–carboxyl hydrogen bonding. Upon dissolution in water, protic redistribution occurs and the complex then behaves as the mono-basic acid Mn(HL)(L). Commensurate with the carboxyl-rich metal environment, metal reduction potentials are high.

Acknowledgements

Crystallography was carried out at the National Single Crystal Diffractometer Facility at the Department of Inorganic Chemistry, IACS. Financial support received from the Department of Science and Technology, New Delhi, is acknowledged.

References

Brauer G (ed.) 1965 *Handbook of preparative inorganic chemistry* (New York: Academic Press) vol. 2, p. 1469
Chandra S K, Basu P, Ray D, Pal S and Chakravorty A 1990a *Inorg. Chem.* **29** 2423
Chandra S K and Chakravorty A 1991 *Inorg. Chem.* **30** 3795
Chandra S K, Choudhury S B, Ray D and Chakravorty A 1990b *J. Chem. Soc., Chem. Commun.* 474
Christou G 1989 *Acc. Chem. Res.* **22** 328
Dismukes G C 1988 *Chim. Scr.* **A28** 99
Drew M G B, Mathews R W and Walton R A 1970 *J. Chem. Soc.* (*A*) 1405

Dutta S, Basu P and Chakravorty A 1991 *Inorg. Chem.* **30** 4031
Fürst W, Gouzerh P and Jeannin Y 1979 *J. Coord. Chem.* **8** 237, and references therein
Guiles R D, Zimmermann J -L, McDermott A E, Yachandra V K, Cole J L, Dexheimer S L, Britt R D, Weighardt K, Bossek U, Sauer K and Klein M P 1990 *Biochemistry* **29** 471
Loiseleur P C S Et H 1973 *Acta Crystallogr.* **B29** 1345
Martell A E and Smith R M 1974 *Critical stability constants* (New York: Plenum) vol. 1, p. 377
Nathan L C, Zapien D C, Mooring A M, Doyle C A and Brown J A 1989 *Polyhedron* **8** 745
North A C T, Philips D C and Mathews F S 1968 *Acta Crystallogr.* **A24** 351
Quaglieri P P and Thomas H L E G 1972 *Acta Crystallogr.* **B28** 2583
Sheldrick G M 1988 SHELXTL-PLUS 88, *Structure determination software programs*, Nicolet Instrument Corporation, 5225-2 Verona Road, Madison, WI 53711
Yamaguchi K and Sawyer D T 1985 *Inorg. Chem.* **24** 971